PERFORMANCE INVESTIGATION OF CAN TYPE GAS TURBINE ENGINE COMBUSTION CHAMBER USING CFD

Prashanth T

Final year under graduate student, Department of Mechanical Engineering,
KCG College of technology, Chennai.
prashanth.astromech@gmail.com

Abstract — **The objective of this paper is to numerically study the role of combustion aerodynamics on the combustion process of CAN TYPE Gas turbine engine combustion chamber. The static conditions of the combustor and the flow streamed pattern of air-fuel mixture are largely influenced by a series of holes drilled on the flame tube. An effective geometrical pattern of these holes is required to have an efficient combustion. Numerical method is used to study and find the optimal geometric pattern and number of holes on flame tube which suits the design requirements. Two combustors with different geometrical pattern of holes were designed. Numerical modeling is done using non-premixed combustion species method of ANSYS fluent 12.0. Propane (C_3H_8) is used as combustion fuel for numerical investigation.**

Index terms: **CAN type combustor, combustor aerodynamics, Flame tube, combustion.**

I. INTRODUCTION:

Gas turbine engine is a type of internal combustion engine that uses air as the working fluid. The gas turbine engine works on the principle of open Brayton cycle. The gas turbine engines find its application in various fields such as aircraft industry, marine industry, power generation etc... The gas turbine engines have revolutionalized the lifestyle of humans by their effective application in the above fields. The effective design of a gas turbine engines in order to have optimum performance and reduced emissions have posed a challenge for the gas turbine researchers over the decades. However the availability of modern design and analysis tools has allowed an effective design of gas turbine engine and a better understanding of combustion chemistry.

1.1 The objectives of the combustor:

1. Completely combust the fuel and minimize the production of NO_X Gases
2. Low pressure loss across the combustor and lower exit temperature profile.
3. The flame must be held inside the combustor during various operating condition.

II. DESIGN OF COMBUSTOR:

The combustion chamber used for this particular analysis is Can type combustion chamber. This type was chosen because of its simple geometry and its performance is in par with the other combustion chambers. Usually in Can type combustion chamber, the air enters the combustor axially. But in this design the air is made to enter radially and the distribution of air across the annulus is determined using CFD. The penetration of air across the liner walls in the different zones and their corresponding effect on combustion is analyzed. The combustor is designed in such a manner that the pressure loss across the length of the combustor is minimum. The pressure loss across the combustion chamber is influenced by two main factors:

1. Skin friction and turbulence
2. Rise in temperature due to combustion.

Two types of flame tube are designed with two different number and size of holes on it. The influence of these holes on the static pressure, temperature across the combustor and the resulting exit velocity is studied in this paper. The effective hole area for both the flame tubes is constant.

2.1 Calculations:

The inlet mass flow rate and temperature from the compressor is assumed as follows:

m_3	0.645 kg/s
T_3	360 K
P_3	219600 N/m^2
P_2-P_1/q_{ref}	37
P_2-P_1/P_2	0.07
R	287 Nm/KgK
A/F ratio (Stochiometric conditions)	15.5:1

Dimension of casing	**Dimension of the flame tube**	**Effective hole area**	**Length of Flame tube**
$A_{ref}= \frac{R\,x\,(m3T3^{0.5})^2\,x(P3-P2)\,x\,(P3-P2)}{2\,x\,P3\,x\,qref\,x\,P3}$	$A_L = K_{opt}$ x A_{ref}	$A_{eff} = \frac{Aref}{\frac{((P3-P2)-Pdiff)^{0.5}}{qref}}$	$L= \frac{combustor\ volume}{area\ of\ snout}$
Aref = [287 x {(0.645 x (360)}0.5 x 37 x 14.285]0.5	= 0.74 x 0.0153	$= \frac{0.0153}{37^{0.5}}$	$\frac{24810}{= 124.05}$
= 0.0153 m^2	= 0.0113 m^2	= 0.0004135 m^2	=200 mm
Rc = 70 mm	R_L = 60 mm.	A_{eff} = 413.5 mm^2	L =200 mm

2.1.1 Flame tube 1 -hole area distribution:

Primary zone holes	**Secondary zone holes**	**Tertiary zone holes**
Distance = 30 mm	Distance = 115 mm	Distance = 170 mm
30% of effective hole area	20% of effective hole area	50% of effective hole area
=124.05 mm^2	=82.7 mm^2	=206.75 mm^2
No. of holes = 16	No. of holes = 4	No. of holes = 4
No of rows = 2	No of rows = 1	No of rows = 1
Area of one hole = 10.33 mm^2	Area of one hole = 20.6 mm^2	Area of one hole =51.6 mm^2
r = 1.8 mm	r = 2.56 mm	r = 4.05 mm

2.1.2 Flame tube 2- hole area distribution:

Primary zone holes	**Secondary zone holes**	**Tertiary zone holes**
Distance = 20 mm	Distance = 125 mm	Distance = 175 mm
30% of effective hole area	20% of effective hole area	50% of effective hole area
=124.05 mm^2	=82.7 mm^2	=206.75 mm^2
No. of holes = 24	No. of holes = 8	No. of holes = 8
No of rows = 3	No of rows = 2	No of rows = 2
Area of one hole = 5.16 mm^2	Area of one hole = 10.33 mm^2	Area of one hole = 25.8mm^2
r = 1.2 mm	r = 1.8 mm	r = 2.8 mm

III. MODELING, MESHING AND BOUNDARY CONDITIONS:

3.1 Modeling:

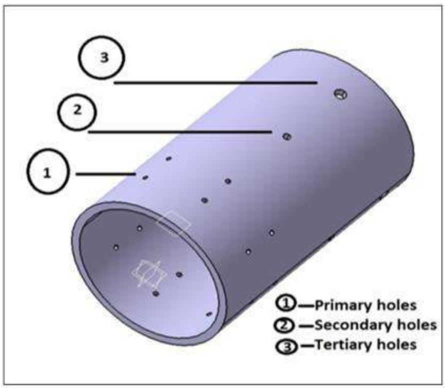

Fig.3.1- Flame tube 1

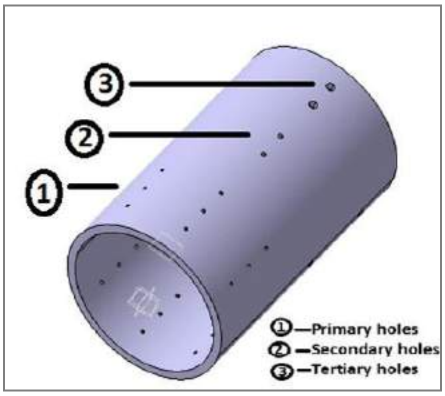

Fig.3.2-Flame tube 2

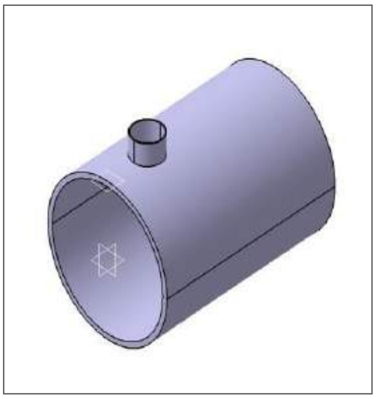

Fig.3.3-Casing

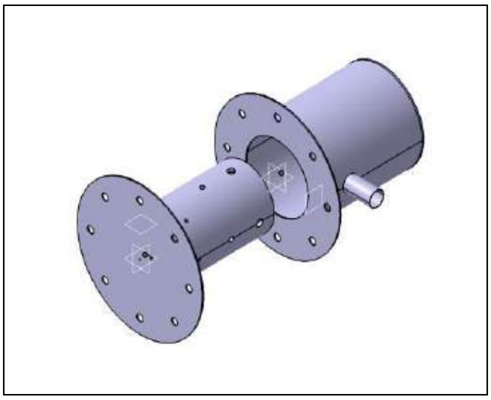

Fig.3.4-Assembly of combustion chamber

Fig.3.5- Exhaust outlet

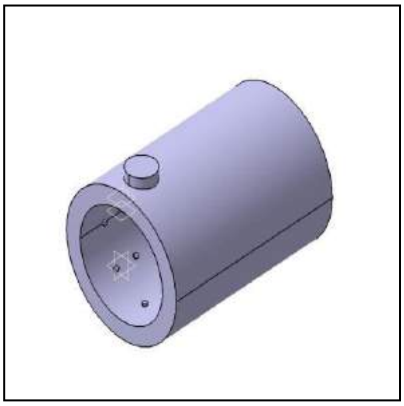

Fig.3.6-Annulus geometry for CFD

3.2 Meshing:

3.2.1 Annulus meshing:

Name	Variables
Type of mesh	Automatic- fine
Element size	1mm
Relevance	30
Mapped face mesh	No
No of nodes	45703
No of elements	235145

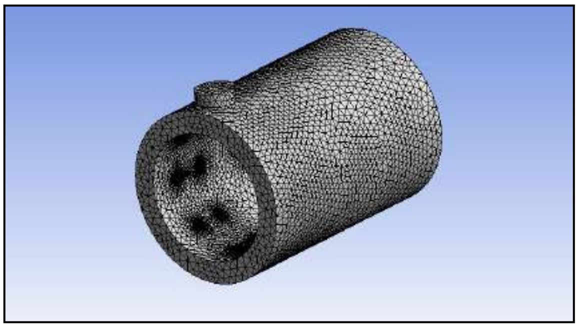

Fig.3.7

The CFD analysis was done for annulus in order to determine the distribution of air across the primary, secondary and tertiary zones. The meshing was done as fine and automatic mesh generation was chosen

3.2.2 Flame tube meshing:

Name	Variables
Type of mesh	Automatic- fine
Solver preference	Fluent
Element edge length	3.65 mm
Smoothing	Medium
No of nodes	65888
No of elements	356819

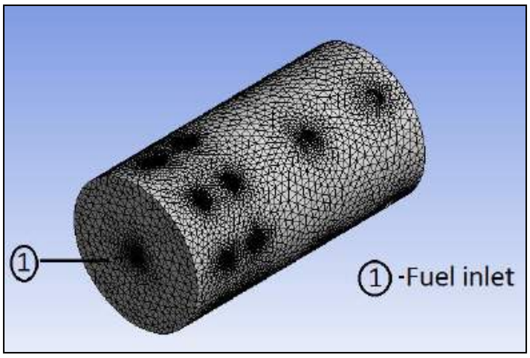

Fig.3.8

Since there is no plane of symmetry for the geometry the flame tube was modeled in 3D as per the dimensions for meshing and analysis. The results were interpreted by creating a plane at the middle of the geometry.

3.3 Boundary conditions:

3.3.1 Annulus boundary condition:

NAME	BOUNDARY CONDITION
Material	Fluid-air
Model	Energy equation, K-£ turbulence
Boundary conditions	Inlet (mass flow inlet) = 0.645 Kg/s, Outlet (Pressure outlet) = 0 pa
Solution initialization	From inlet
No of iterations	500

3.3.2 Flame tube boundary conditions:

NAME	BOUNDARY CONDITION
Material	Pdf mixture
Model	Energy equation, K-£ turbulence, p1 radiation, non-premixed combustion, species-C_3H_8, Pdf table generation
Boundary conditions	Mass flow inlet, pressure outlet =0, mass flow inlet fuel = 0.0416 Kg/s
Solution initialization	Fuel inlet
No of iterations	1000

3.3.2.1 Mass flow inlet (kg/s) for flame tube 1:

HOLE POSITION	ROW 1	ROW 2	ROW 3	ROW 4
Upper hole	0.0165	0.0154	0.0390	0.0956
Lower hole	0.0148	0.0155	0.0420	0.1080

3.3.2.2 Mass flow inlet (kg/s) for flame tube 2:

HOLE POSITION	ROW 1	ROW 2	ROW 3	ROW 4	ROW 5	ROW 6	ROW 7
Upper hole	0.0141	0.0092	0.011	0.029	0.029	0.072	0.069
Lower hole	0.013	0.013	0.011	0.029	0.028	0.069	0.071

The above mass flow rates were calculated based on the velocity across the holes which where obtained during the CFD analysis of annulus.

IV. RESULTS AND DISCUSSIONS:

The CFD analysis was done and the following results were obtained.

4.1 Annulus CFD results:

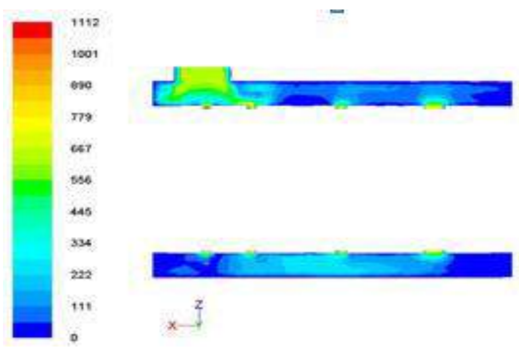

Fig.4.1-Contours of velocity- flame tube 1

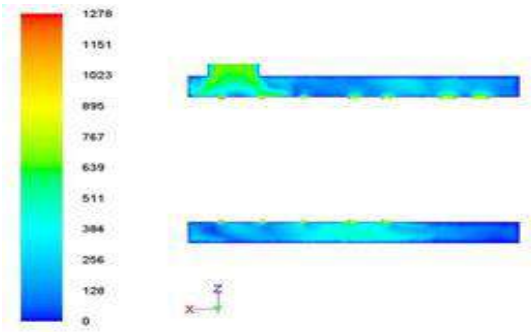

Fig.4.2-Contours of velocity- Flame tube 2

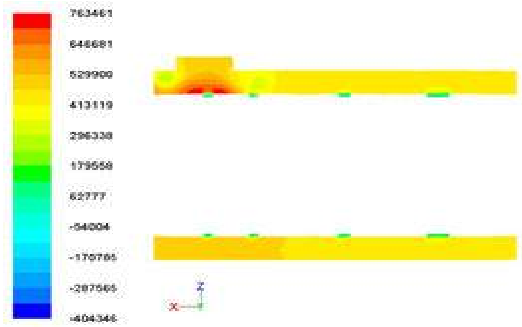

Fig.4.3- Contours of static pressure- Flame tube1

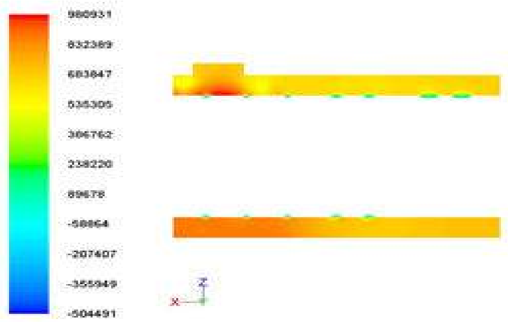

Fig.4.4-Contours of static pressure- Flame tube 2

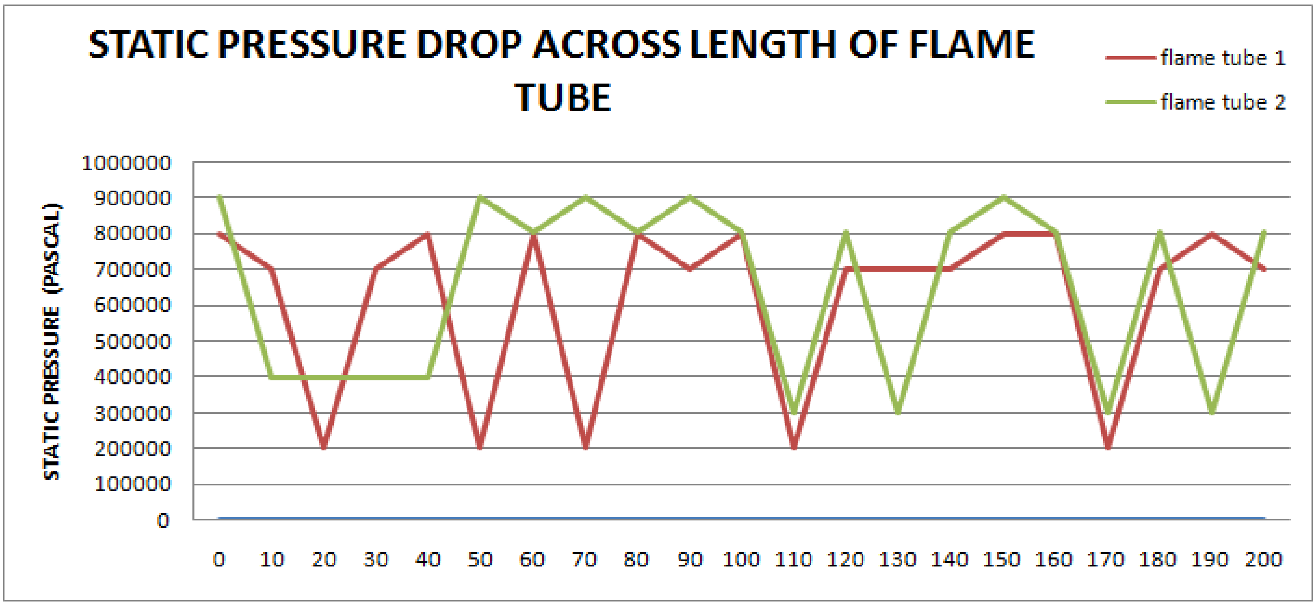

Fig.4.5

4.2 Flame tube CFD results:

CONTOURS FOR FLAME TUBE 1

CONTOURS FOR FLAME TUBE 2

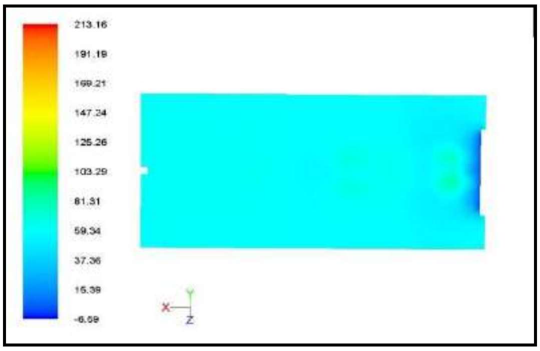

Fig.4.6- Flame tube 1 static pressure contour

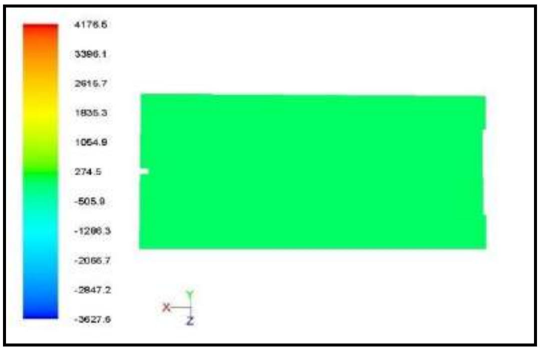

Fig.4.7-Flame tube 2 static pressure contour

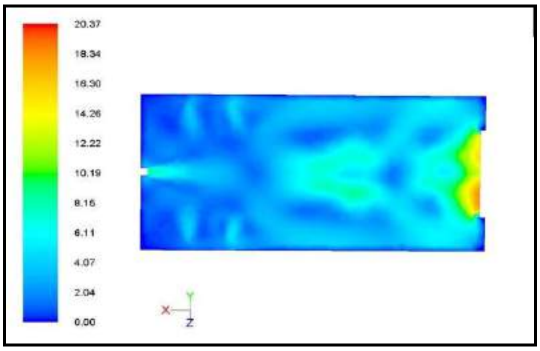

Fig.4.8- Flame tube 1 velocity magnitude contour

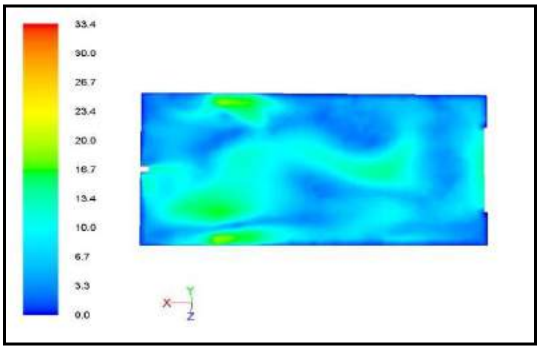

Fig.4.9- Flame tube 2 velocity magnitude contour

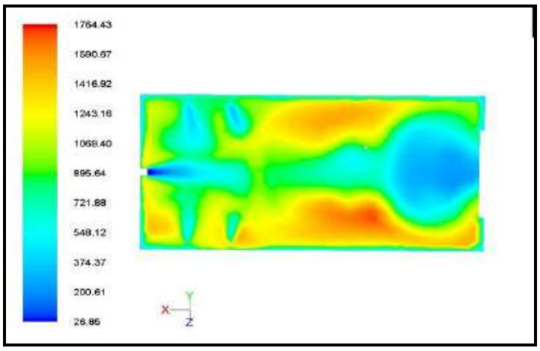

Fig.4.10- Flame tube 1 static temperature contour

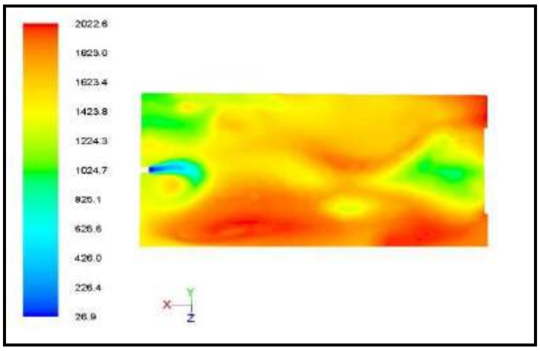

Fig.4.11-Flame tube 2 static temperature contour

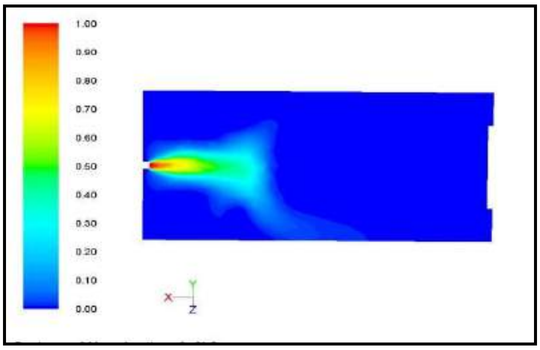

Fig.4.12-Flame tube 1 mass fraction of C_3H_8 contour

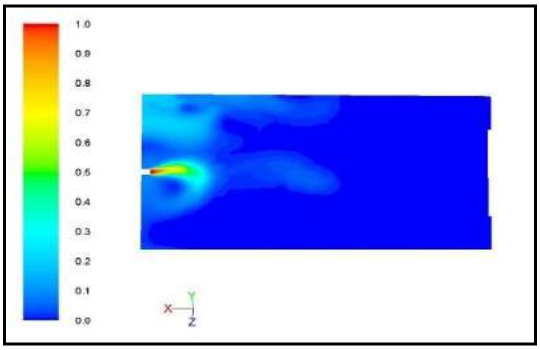

Fig.4.13-Flame tube 2 mass fraction of C_3H_8 contour

GRAPHS OF FLAME TUBE 1

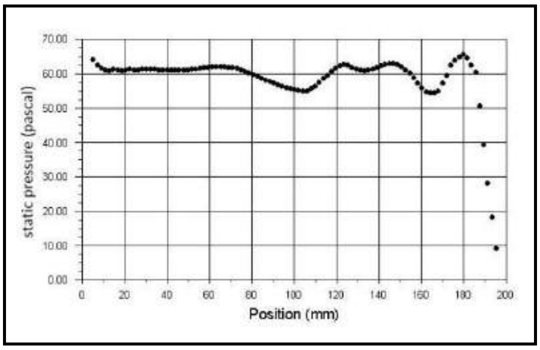

Fig.4.14-Flame tube 1 static pressure graph

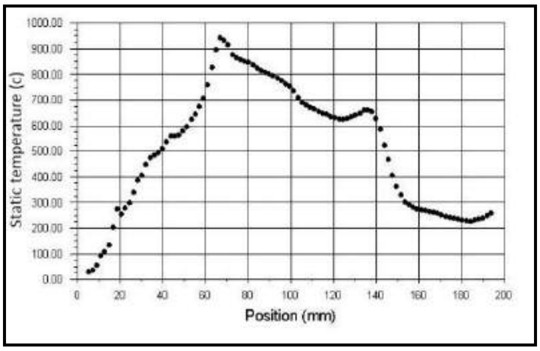

Fig.4.16-Flame tube 1 static temperature graph

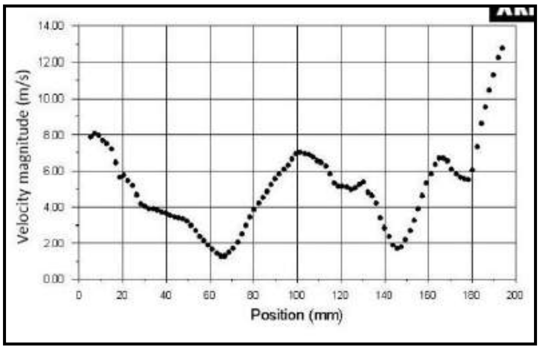

Fig.4.18-Flame tube 1 velocity magnitude graph

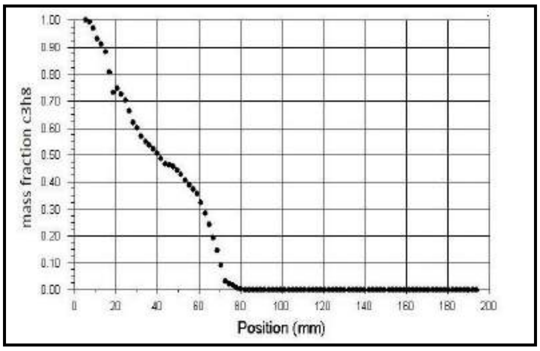

Fig.4.20-Flame tube 1 mass fraction of C_3H_8 graph

GRAPHS OF FLAME TUBE 2

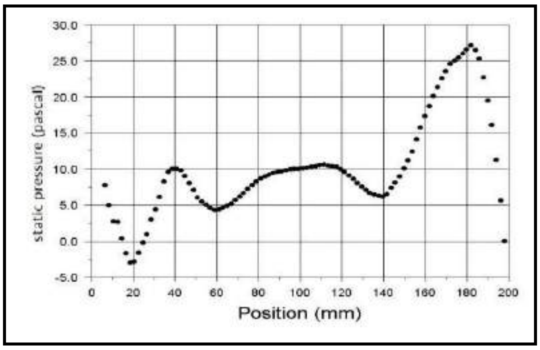

Fig.4.15-Flame tube 2 static pressure graph

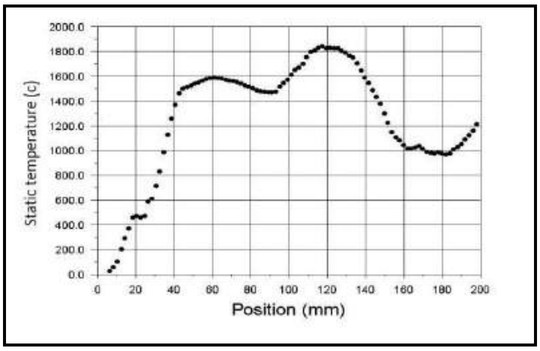

Fig.4.17-Flame tube 2 static temperature graph

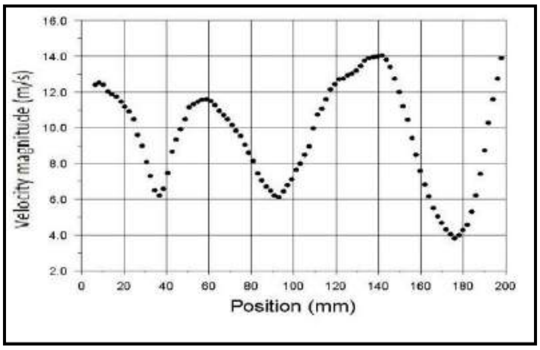

Fig.4.19-Flame tube 2 velocity magnitude graph

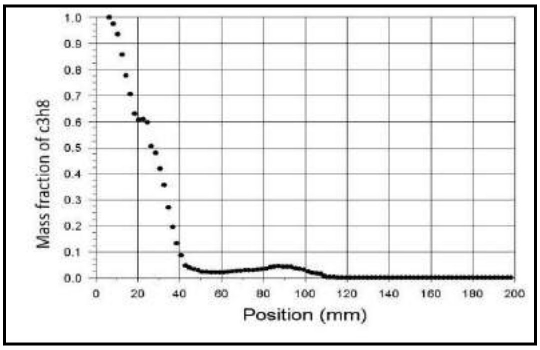

Fig.4.21-Flame tube 2 mass fraction of C_3H_8 graph

	AVERAGE PRESSURE	MAXIMUM TEMPERATURE	MAXIMUM EXIT VELOCITY	MASS FRACTION OF C_3H_8 AT PRIMARY ZONE
FLAME TUBE 1	65 Pa	920ºC	13 m/s	0.1
FLAME TUBE 2	10 Pa	1800ºC	14 m/s	0.02

4.3 Flame tube 1 discussions:

The graph of static pressure illustrates that the pressure loss across the flame tube is almost constant at 65pa. The maximum temperature is around 920ºC which falls in the primary zone. The mass fraction of C_3H_8 is dropping continuously across the flame tube which indicates that the entire fuel is not burnt in the primary zone alone .The deflagration flames propagate till the end of secondary zone. The exit velocity in this case is around 13 m/s. It could also be noted that the temperature of the burnt gases continues to fall after the secondary zone, the reason could be attributed to the influence of the dilution zone holes which effectively dilutes the temperature of burnt gases.

4.4 Flame tube 2 discussions:

It could be inferred from the graph that the static pressure fluctuates rapidly across the length of the flame tube as this could be due to small size holes which injects the air at high velocity. The maximum pressure is only around 10 Pa. The temperature profile across the length of the flame tube is well above 1100ºC with a peak value of 1800ºC. Such high temperatures have robust influence on the density of mixture. There is a precipitous drop in mass fraction of C_3H_8 at a distance of 45mm along the flame tube which clearly indicates that the maximum amount of fuel is mixed with the air in the primary zone. The exit velocity is around 14 m/s.

V. CONCLUSION:

Based on the CFD analysis of two flame tubes with different hole configuration, though the flame tube 2 has better mixing of air and fuel in the primary zone, the temperature is quite high which might cause hotspots on the walls of combustion chamber. On the other hand there is comparatively lower temperature in the flame tube 1 and the static pressure also remains constant across the flame tube, thus contributing to wider flammability limits for the combustor.

Since the exit temperature profile is of significant importance for the turbine blade material, it is always desirable to have lower exit temperature and also there is a primary need to achieve equity among the vital parameters such as static pressure, static temperature and exit velocity. The geometrical hole pattern of flame tube 1 satisfies these requirements which is evident from the analysis. Thus it could be concluded that the design specifications of flame tube 1 is more reliable than flame tube 2.

VI. REFERENCES:

1. “GAS Turbine Combustion Alternative Fuels and Emissions”, third edition by “Arthur H Lefevbre, Dilip R Ballal “.
2. “Gas Turbine Theory”, fourth edition by “H Cohen, CFC Rogers, HIH Saravanamutto”.
3. “Fundamentals of compressible flow”, fifth multicolor edition by “SM Yahya”.
4. ANSYS Fluent 12 “Fluent tutorials for non-premixed combustion”.
5. ANSYS Fluent 12 “Theory guide”.